IEEE Access
Multidisciplinary | Rapid Review | Open Access Journal

Received January 21, 2019, accepted February 7, 2019, date of publication March 4, 2019, date of current version March 13, 2019.

Digital Object Identifier 10.1109/ACCESS.2019.2901286

Multi-Spectral Image Change Detection Based on Band Selection and Single-Band Iterative Weighting

LIYUAN MA[1], ZHENHONG JIA[1], YINFENG YU[1], JIE YANG[2], AND NIKOLA K. KASABOV[3], (Fellow, IEEE)

[1]College of Information Science and Engineering, Xinjiang University, Ürümqi 830046, China
[2]Institute of Image Processing and Pattern Recognition, Shanghai Jiao Tong University, Shanghai 200400, China
[3]Knowledge Engineering and Discovery Research Institute, Auckland University of Technology, Auckland 1020, New Zealand

Corresponding author: Zhenhong Jia (jzhh@xju.edu.cn)

This work was supported in part by the National Science Foundation of China under Grant 61665012 and Grant U1803261, in part by the International Science and Technology Cooperation Project of the Ministry of Education of the People's Republic of China under Grant DICE 2016–2196, and in part by the Natural Science Foundation of Xinjiang under Grant 2015211C288.

ABSTRACT Iteratively reweighted multivariate alteration detection algorithm has the phenomena of broken patches, much noise, and small change area that are difficult to detect, and the overall detection rate is low. In order to solve this problem, this paper proposes a multi-spectral image change detection algorithm based on band selection and single-band iterative weighting. Because the change information of the multi-spectral image is concentrated in some bands, the background and noise information of the rest bands are more, which may have a negative effect on the final result. Therefore, the band with more change information is selected first, and the iterative weighting of a single band can better suppress the noise and background information, so as to obtain a higher band correlation and facilitate the extraction of change information. This method is used to obtain the characteristic difference graph of the selected band with more change information. After Gaussian denoising of each characteristic difference graph, the Euclidean distance formula is used to fuse the difference graph of each band into a change intensity graph. Finally, the unsupervised k-means clustering algorithm is used to perform binary-valued clustering on the fused difference graph to obtain the change detection results. As a practical application, the superior performance of our proposed method was demonstrated through a large number of comparative tests.

INDEX TERMS Multi-spectral change detection, IR-MAD, band selection.

I. INTRODUCTION

Remote sensing image change detection technology has been applied in many fields, such as environmental monitoring [1], urban research [2], land use [3], [4], sand cover monitoring [5], forest monitoring [6], [7], agricultural investigation [8], disaster assessment [9] and so on. The change detection of remote sensing images is based on the multiple remote sensing images acquired at different time points in the same region to extract the feature and process of the change of ground objects [10]. There are different structures and compositions of ground objects that make different ground objects have different spectral features, that is, the reflection spectrum curves of different ground objects are different. If the reflectance spectra of different objects are similar in some bands, the reflectance spectra of these objects in other bands will greatly differ. Single-band remote sensing image change detection can identify the object in a band, but cannot extract the features in other wavelength change information. Furthermore, the multi-spectral remote sensing images of multiple wavelengths can reflect the characteristics of features under different wave bands, and make good use of spectrum correlation. Moreover, the difference can be more realistic, as well as the change in reaction features [11].

Due to the use of multi-spectral images for change detection, abundant spectral information can improve the credibility of identifying multiple types of changes. Hence, some

The associate editor coordinating the review of this manuscript and approving it for publication was Ke Gu.

targets that cannot be detected in a single band can more likely to be detected in multiple bands, and this would be more conducive to understanding the change information of ground objects. The most critical part of change detection is change information discovery, and most studies have ventured around this issue [12]. In order to solve the deficiency of single-band change detection methods, such as the image ratio method [13], change vector analysis (CVA) [14], and principal component analysis (PCA) [15], in multi-band remote sensing image change detection (suppressing noise, improving detection accuracy, etc.), Bai *et al.* [16] took the lead in proposing the concept and method of multivariate job-detection (MAD). The MAD algorithm is based on the Canonical Correlation Analysis (CCA) [17]. Liao *et al.* [18] applied this method to the multi-temporal and multi-band remote sensing image change detection, and the experimental results revealed the obvious advantages and application potential of this method. However, the algorithm could still not fully improve the deficiency of noise suppression and accuracy improvement in the present multivariate remote sensing image processing. Based on the MAD method, Canty and Nielsen [19] also proposed the iterative weighted multivariate tissue detection (iteratively reweighted-MAD, IR-MAD). A subsequent literature [20] has proven that nuclear principal component analysis and nuclear MAF (the largest correlative factor) can further enhance the IR-MAD results after the implementation of IR-MAD. In [21], the application of IR- MAD on image fragments, rather than on pixels, was demonstrated. In another study [22], the IR-MAD method was proposed to eliminate strong changes to improve these results. By eliminating strong changes with a mask, the algorithm could better identify the background without changes. Although the iteration time and detection accuracy were improved, these still could not make full use of the variation information of each band.

The IR-MAD algorithm has been considered as the most advanced change detection algorithm of a multiphase satellite due to its excellent change in detection accuracy and varying stability. By chi-square distribution probability, the method to simulate the probability of each pixel did not induce change to calculate the weight. In the next iteration, the calculation of the mean and variance were considering weight. Through this, the unchanging pixels were given higher weights. Furthermore, with the use of the weights of the size of the difference between changed and unchanged pixels, the iterative convergence was able to obtain more accurate change detection results. Another theoretical explanation for IR-MAD was proposed in [23]: multivariate change detection is the feature that seeks the strongest image correlation. This algorithm makes full use of the band with a strong correlation, while the band with a weaker correlation is given a lower weight, which contributes less to the calculation of variation strength. Therefore, the IR-MAD algorithm fails to make full use of the variation characteristics of each wave band, resulting in the incomplete detection of the variation areas of details. Therefore, the algorithm has broken patches, much noise, and small change areas that are difficult to detect, and the overall detection rate is low [24].

Through the study of the above problems, a new improved IR-MAD method was proposed for the detection of multi-spectral image changes. This algorithm selects the bands with strong correlation by calculating the correlation of each band. After a lot of experiments and comprehensive consideration of detection accuracy and time complexity, this paper selects three bands for change detection. The selected bands are sequentially subjected to single-band iterative weighting, and different weights are set for the images of the respective bands, which better improves the correlation between the pairs of the multi-spectral images. This method is used to obtain the characteristic difference graph of each wave band with more change information. Because the noise of multi-spectral image is mainly additive noise (such as Gaussian noise, Poisson noise, etc.), Gaussian denoising algorithm is selected in this paper for simple denoising of each feature difference graph. After Gaussian denoising of each characteristic difference graph, the Euclidean distance formula is used to fuse the difference graph of each wave band into a change intensity graph. Finally, unsupervised k-means clustering [25] was carried out to obtain the change detection results. Landsat image data set was used for experiments, and the processing results proved the superiority of the proposed method. Meanwhile, the detection results of MAD, IR-MAD and the later published IR-MAD algorithm using mask to eliminate strong changes were compared, and the results showed that the proposed method had higher detection accuracy of changes. Finally, the proposed method was discussed in terms of time complexity and universality.

II. THEORETICAL ANALYSIS

A. BAND SELECTION

Since the variation information is concentrated in some bands for multi-spectral images, while the background and noise information of other bands are more, which may have negative effects on the final result. Selecting a certain number of wavebands that contain a lot of change information and conducting change detection is conducive to the accurate extraction of change information and the reduction of time complexity.

The IR-MAD algorithm outputs characteristic bands in the order of correlation coefficients from small to large. Fig. 1 (a) is the RGB image synthesized by the first three characteristic bands. Fig. 1(b) is a composite RGB image of the last three characteristic bands. Through observation can find, row in front of the characteristic difference value of the band with small correlation coefficient contains more noise and background information. Row in the back of the band with large correlation coefficient contains more change information, noise is also less. It can be find that the band having a greater value of the characteristic correlation ρ contains more variation information. Therefore, the characteristic canonical correlation between remote sensing image wavebands can

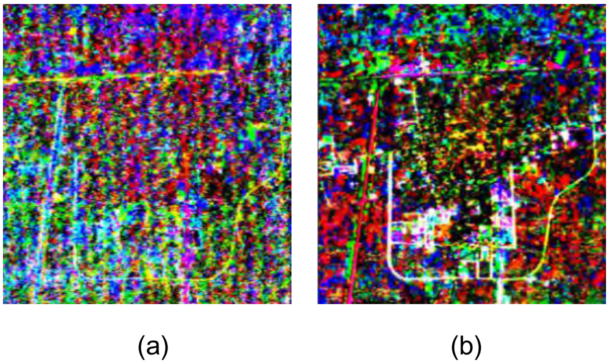

FIGURE 1. Color synthesis map of the first three characteristic bands of the IR-MAD algorithm;(b) Color synthesis map of the last three characteristic bands of the IR-MAD algorithm.

be calculated to obtain the wavebands with more changing information for band selection. The calculation of ρ is as follows:

Suppose that for the same scene, two multi-spectral images F and G of k-bands are obtained at two different times. We can express the observation results in different bands of multi-spectral images as random vectors $F_1, F_2, F_3 \ldots F_K$ and $G_1, G_2, G_3, \ldots G_K$. Let a and b represent the projection vectors of F and G, respectively. The projection vectors of F and G are expressed as U and V respectively:

$$U = a^T F = a_1F_1 + a_2F_2 + \ldots + a_KF_K \tag{1}$$
$$V = b^T G = b_1G_1 + b_2G_2 + \ldots + b_KG_K \tag{2}$$

The characteristic correlation coefficient ρ can be expressed as:

$$\rho = Corr\left(a^T F, b^T G\right) = \frac{Corr\left(a^T F, b^T G\right)}{\sqrt{Var(a^T F)Var(b^T G)}} \tag{3}$$

The variance and covariance of U and V can be calculated as:

$$Var\ (U) = a^T \sum\nolimits_{FF} a \tag{4}$$
$$Var\ (V) = b^T \sum\nolimits_{GG} b \tag{5}$$
$$Corr\ (U, V) = a^T \sum\nolimits_{FG} b \tag{6}$$

where $\sum_{FF}$ is the covariance matrix of the first graph, $\sum_{GG}$ is the covariance matrix of the second graph, $\sum_{FG}$ and $\sum_{GF}$ is the covariance matrix between two images. The constraint condition is: Var $\left(a^T \mathrm{F}\right) = 1$, Var $\left(b^T \mathrm{G}\right) = 1$. The projection vectors a and the characteristic correlation ρ can be found through Eq. (7)

$$\sum\nolimits_{FF}^{-1} \sum\nolimits_{FG} \sum\nolimits_{GG}^{-1} \sum\nolimits_{GF} a = \rho^2 a \tag{7}$$

Is equivalent to obtain the eigenvalues and corresponding eigenvectors of $\sum_{FF}^{-1} \sum_{FG} \sum_{GG}^{-1} \sum_{GF}$, respectively corresponding to ρ^2 and a, then the characteristic correlation coefficient ρ can be obtained. By arranging the characteristic canonical correlation coefficients between the bands of remote sensing images obtained by calculation from large to small, the order of change information from more to less can be obtained.

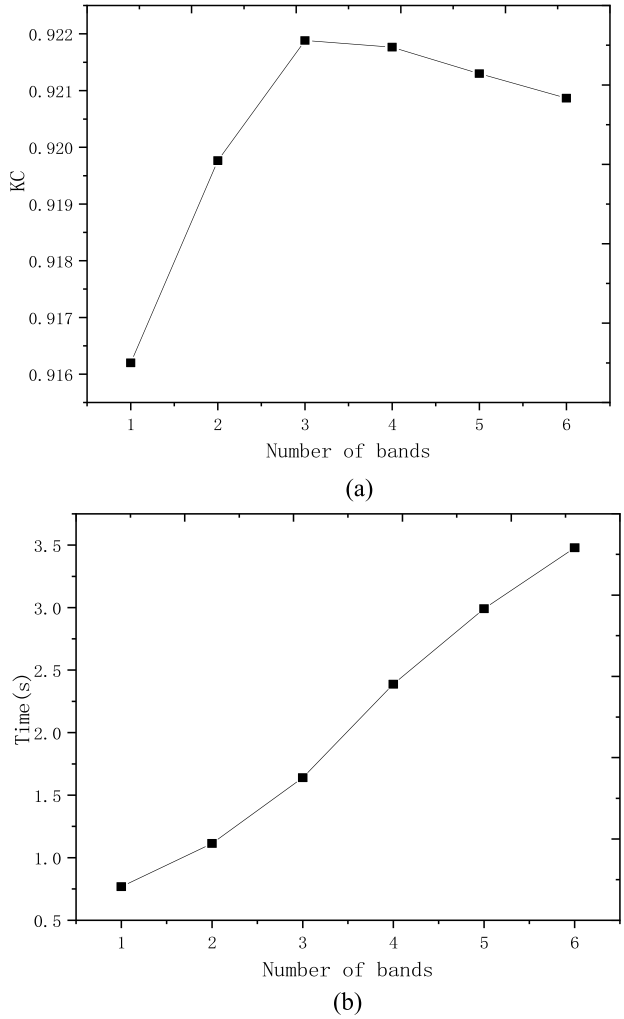

FIGURE 2. (a) The relationship between the number of selected bands and KAPPA values; (b) The relationship between the number of bands selected and the time complexity.

In this paper, 5 sets of multi-spectral data sets are used, which includes a set of Taizhou ETM+ data with the size of 400 × 400 and 4 sets of Changji landsat5-Tm data sets were made by manually adding change areas with a size of 500 × 500 (The specific method of adding the change area is as shown in the data I). And the number of 1-m(m = 1, 2, 3, 4, 5, 6) bands after sorting is taken to carry out the experiment with the same number of 10 iterations. Take the mean value of the results of 5 groups of data, and make the relationship diagram between the selected number of bands and the KAPPA value and time complexity, as shown in Fig. 2 (a) and (b). According to (a) in Fig. 2, KAPPA value is the highest when the number of selected bands is 3, and then decreases slightly with the increase of the number of selected bands; According to (b) in Fig. 2, the time complexity increases with the increase of the number of bands selected. From 3 bands to 4 bands, the slope is the largest and the time increase is the largest. Therefore, after comprehensive consideration of detection accuracy and time complexity, this paper selects three bands for change detection.

B. SINGLE BAND ITERATIVE WEIGHTING ALGORITHM

The idea of single-band iterative weighting is as follows: First, the single-band image is extracted from the multi-spectral image. Second, the image is individually weighted by iteration for each band to obtain a projection vector that maximizes the correlation coefficient of each band image. Then, the optimal MAD variable of the band is obtained. In this way, the obtained MAD variables have the most abundant change information in each band. Third, the final change intensity map is generated after the fusion of the change intensity. The specific implementation method is as follows:

First, extract a single band image in the multispectral image $F_1, F_2, \ldots F_K$, and a single band image in the multispectral $G_1, G_1, \ldots G_K$.

Second, a projection vector that maximizes the correlation coefficient of each band image is found. Let the vector of the Pth band image be optimally projected as U_P and V_P, as shown in Eq. (8) and (9):

$$U_P = a_P^T F_P \tag{8}$$

$$V_P = b_P^T G_P \quad P = 1 \ldots K \tag{9}$$

where P is the corresponding number of bands, and a_P and b_P represent the projection vectors of the F and G p-band images, respectively. The projection vectors a_P and b_P can be found through Eq. (10) and (11):

$$\sum\nolimits_{F_P G_P} \sum\nolimits_{G_P G_P}^{-1} \sum\nolimits_{G_P F_P} a_P = \rho^2 \sum\nolimits_{F_P F_P} a_P \tag{10}$$

$$\sum\nolimits_{G_P F_P} \sum\nolimits_{F_P F_P}^{-1} \sum\nolimits_{F_P G_P} b_P = \rho^2 \sum\nolimits_{G_P G_P} b_P \tag{11}$$

where $\rho = \mathrm{Corr}(a_P^T F_P, b_P^T G_P)$ represents the correlation of two eigenvectors. $\sum_{F_P F_P}$ is the covariance matrix of the P-band image of the multi-spectral image F. $\sum_{G_P G_P}$ is the covariance matrix of the P-band image of the multi-spectral image $\sum_{F_P G_P}$ and $\sum_{G_P F_P}$ is the cross-covariance matrix between two P-band images. The MAD variable M_P generated by a single band is expressed, as shown in Eq. (12):

$$M_P = U_P - V_P = a_P^T F_P - b_P^T G_P \tag{12}$$

The MAD feature satisfies the properties of the Gaussian distribution. Hence, the chi-square distance of the difference image can be calculated, which satisfies the chi-square distribution with a degree of freedom n, as shown in Eq. (13):

$$T_{ij} = \left(\frac{M_{ij}^P}{\sigma^P} \right)^2 \in x^2(n) \tag{13}$$

where σ^P is the variance of the P-th band, and the weight is calculated by the probability density quantile of the chi-square distribution:

$$\omega_{ij} = P\left(T_{ij} > t\right) = P\left(x^2\,(n) > T_{ij}\right) \tag{14}$$

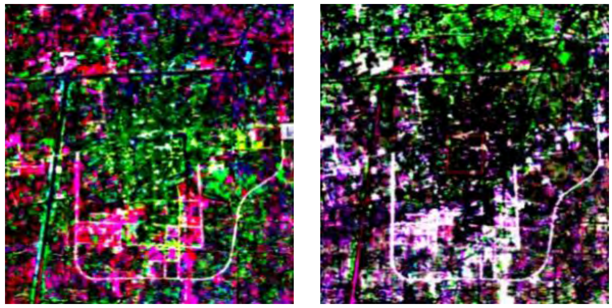

(a) (b)

FIGURE 3. Color synthesis map of the single-band iterative weighting algorithm: (a) shows the RGB image synthesized by band 3, band 4 and band 5; (b) shows the RGB image synthesized by band 6, band 2 and band 1.

In the next iteration of the corresponding p-band image, the calculation of the mean and variance takes into account the effect of the weight. That is, the image of each band uses the respective correlation coefficients to find the projection vector and weight in the iterative calculation process. As shown in the Eq. (12), the variation intensity matrix is calculated. After iterative convergence, the optimal MAD variable of P-band can be obtained. The best difference image M_P of each band can be obtained through this algorithm. After Gaussian filtering and denoising, the obtained difference matrix is adjusted into the column vector and written by band in matrix M as shown in the Eq. (15):

$$M = (M_1, M_2, \ldots M_K) \tag{15}$$

$$MAD = \sqrt{\sum\nolimits_{K=1}^{P} (M \cdot M)} \tag{16}$$

Third, the Euclidean distance (such as Eq. (16)) is used to convert the difference matrix into the change intensity matrix MAD, and the intensity of the change of the pixels in each band is unified.

Fig. 3 (a) is the RGB image synthesized by band3, band4 and band5. Fig. 3 (b) is the RGB image synthesized by band6, band2 and band1 (the same band used in Fig. 1). Figure 4 is the phase relationship values of each band obtained after 10 iterations of IR-MAD algorithm and single-band iterative weighting method respectively adopted in data II. Comparing (a) in Fig. 1 with (a) in Fig. 3, it can be seen that the color composite map in which the original change information is blurred becomes clear. The single-band iterative weighting method significantly enhances the correlation of the weakly correlated band 3, band 4, and band 5. The histogram in Fig. 4 is also a good proof of this. Therefore, the single-band iterative weighting method can well enhance the correlation coefficient of each band and realize the minimization of the radiation differences contained in the unchanged pixel, so as to minimize the radiation difference in the difference values and highlight the real changing ground objects.

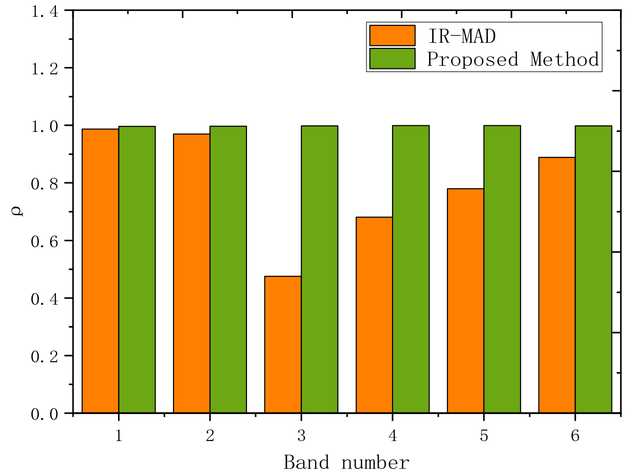

FIGURE 4. IR-MAD algorithm and the algorithm in this paper after the processing of each band correlation value.

C. ALGORITHM IMPLEMENTATION STEPS AND FLOW CHART

The algorithm in the present study comprises of five steps:

Step1. The original multi-spectral image was calibrated by ENVI software, and the single-band image was separated;

Step2. The Eq. (7) is used to calculate the characteristic correlation between band pairs, and the first three bands with strong correlation are selected for change detection;

Step3. For the selected wave band, the optimal projection vector maximized by relation number was obtained by iterative weighting of single wave band. The weight was calculated by Eq. (14), and the optimal projection vector was calculated by Eq. (10-11). The differential images of each band were obtained by using Eq. (12), and gaussian denoising was performed;

Step4. The Eq. (15) is used to write the filtered difference image of each band into a matrix, and the Euclidean distance Eq. (16) converts the difference matrix into a change intensity matrix with the same change intensity;

Step5. K-means is used for binary clustering analysis to obtain the change detection results.

The flow chart is shown in Fig. 5:

III. EXPERIMENTAL RESULTS

In order to verify the superiority of the proposed algorithm, three different landsat datasets were selected for the experiments. The detection results obtained by different algorithms were compared from subjective and objective indicators. The objective indicators included the false negative (FN), false positive (FP), overall error (OE), percentage correct classification (PCC) [26], and Kappa coefficient (KC) [27], time complexity. FN indicates the number of pixels that are originally detected as a change class, and is detected as a change class, which is called a missed check number; FP

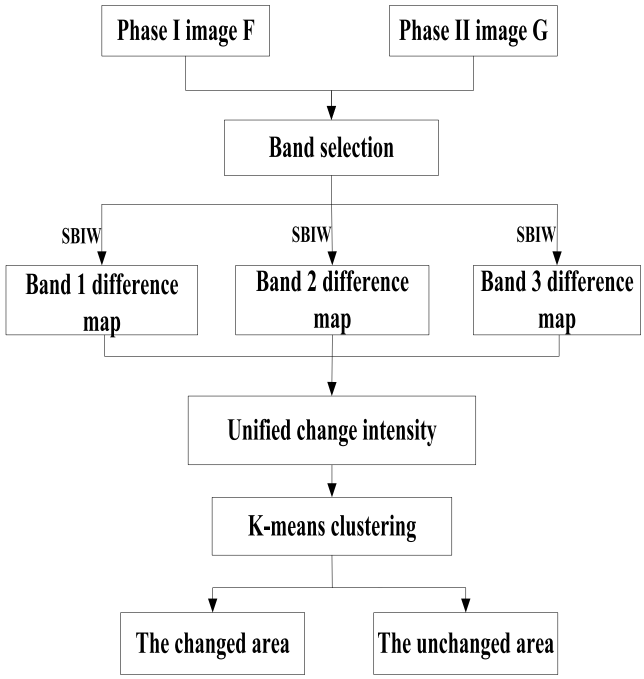

FIGURE 5. The algorithm flow chart.

indicates the number of pixels that are originally detected as a change class, which is an unchanging class, and is called a misdetection number; OE represents the sum of the number of false alarms and missed detections; PCC indicates the proportion of correctly classified samples to the total number of samples. The closer the PCC is to 1, the better the change detection performance. KC is a more accurate measurement of classification accuracy. The value of the parameter is usually used to measure the similarity between the change result graph and reference image. The ideal value is 1, which means that the test result is completely consistent with the reference image [28]. Time complexity refers to the time used for algorithm implementation. In order to reduce the experimental error, the time complexity calculated in this paper takes the average of the results of 10 runs.

A. EXPERIMENTAL DATE I

Data I was conducted with artificial simulated data. The remote sensing image of phase 1 was taken by landsat5-TM [29] in 2011, and it is a multi-spectral image of changji region in xinjiang; The remote sensing image of phase 2 is simulated by manually adding changing regions to the multi-spectral remote sensing image of phase 1.The specific adding method is as follows: A region of A of a certain size is captured from the Band 1 image, and A is replaced by region B, which contains different ground object information (A is the same size as B and contains different ground object information) to simulate the changing region. This method is used to obtain the Band 1 images of time phase two, and process the remaining bands equally (the positions of the intercepting and replacement regions are completely consistent with Band 1). In this way, the single-band processing can

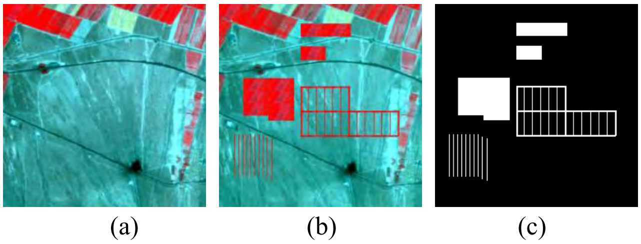

FIGURE 6. (a) Pseudo-color composite image of the multispectral data. (b) Pseudo-color composite image of (a) the multispectral data change simulation. (c) The reference change image.

guarantee the consistency of ground features of each band. Then, the simulated time-phase two multispectral images can be obtained. The obtained multi-temporal landsat multispectral image has many advantages. (1) It is not affected by clouds, weather, etc.. Hence, registration is not required. (2) Since the pixel values are completely consistent, except for the change area, the detection is almost free from noise. (3) As the change area is manually added, it is convenient to make the change reference graph for the objective analysis of the test results. Therefore, the simulation of multispectral image change in this manner can be used to detect the advantages and disadvantages of the algorithm. Fig. 6 (a) shows the pseudo-color composite image of the multi-spectral data in the Changji area of Xinjiang in 2011, and the images are 250×250 pixels. Fig. 6 (b) shows the pseudo color composite image after manually adding the change area to Fig. 6 (a). The change reference map is presented in Fig. 6 (c).

The data set was used to carry out the change detection experiment, and was compared with the MAD algorithm, IR-MAD algorithm, and the mask removal strong change method. At the same time, in order to verify the advantages of band selection, the proposed method was compared with the K-means clustering and Fuzzy C-means (FCM) clustering using the single-band iterative algorithm in the case of no band selection. The experimental results are shown in Fig. 7:

It can be seen from the observation in Fig. 7 that the proposed method has obvious advantages over the MAD algorithm, the IR-MAD algorithm and the masking elimination method, there is less noise in the detection results, and the detected change area is more complete. The two comparison algorithms of the single-band iterative weighting algorithm are similar to the detection results of the proposed method. By observing the objective evaluation index Table 1, it can be seen that the total number of missed detection FN and false alarm FP after band selection is lower, and the accuracy of PCC and KAPPA values are also improved, indicating that the detection accuracy can be improved after band selection. In terms of time complexity, the MAD algorithm does not need iteration and has the lowest time complexity. But in terms of accuracy PCC and KAPPA values, MAD algorithm has low detection accuracy. The proposed method has low time complexity and the highest accuracy, so it has better change detection ability.

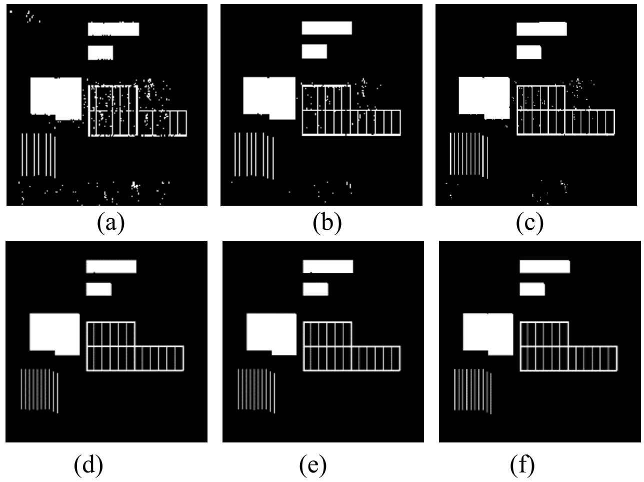

FIGURE 7. Change detection image obtained for the Changji simulated data set: (a) MAD; (b) IR-MAD; (c) masking to eliminate strong changes; (d) Single-band iterative algorithm and K-means clustering were used in the case of no band selection;(e) Single-band iterative algorithm and FCM clustering were used in the case of no band selection;(f) Proposed method.

TABLE 1. The multi-spectral image change detection results evaluated by different algorithms.

Method Used	OE	PCC(%)	KC	Time(s)
MAD	715	0.988	0.939	0.242
IR-MAD	208	0.996	0.982	0.686
With Mask	185	0.997	0.984	0.978
SBIW(k-mean)	14	0.999	0.998	0.482
SBIW(FCM)	14	0.999	0.998	0.578
Proposed Method	6	0.999	0.999	0.244

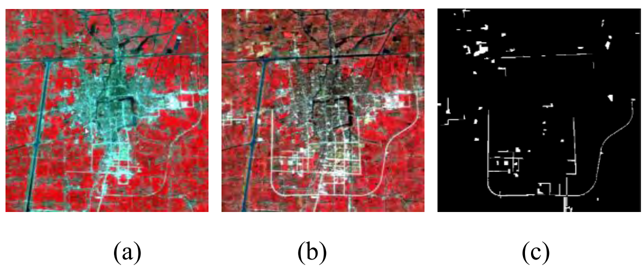

FIGURE 8. Taizhou ETM+ data pseudo-color composite image: (a) 2000 and (b) 2003; (c) Test sample of the Taizhou image. The background samples were black, the unchanged samples were gray, and the change samples were white.

B. EXPERIMENTAL DATE II

Data II was the real multispectral remote sensing data of Taizhou city. The data sets was acquired on March 17, 2000 and February 6, 2003, respectively. The shooting area was located in Taizhou City, Jiangsu Province, China. The image size was 400×400, including six band pixels. The two remote sensing images shown in Fig. 8 (a) and Fig. 8 (b) comprised of Band 4 (red band), Band3 (green band), and Band 2 (blue band) pseudo color synthesis. The change reference map is presented in Fig. 8 (c).

By observing the change detection results in Fig.9, it can be seen the detection result of MAD algorithm is the worst.

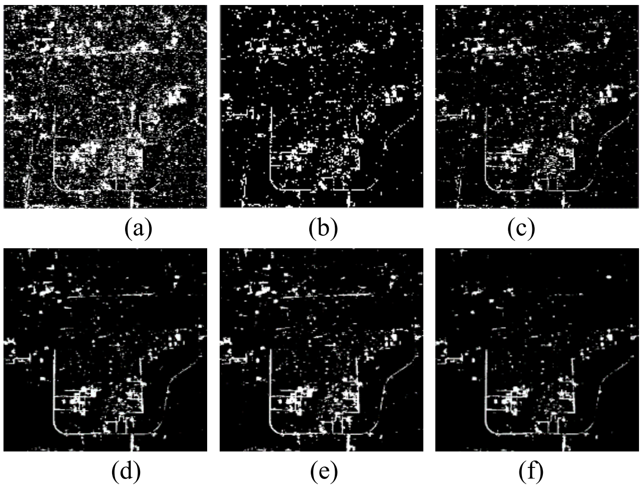

FIGURE 9. Change detection image obtained for the Changji simulated data set: (a) MAD; (b) IR-MAD; (c) masking to eliminate strong changes; (d) Single-band iterative algorithm and K-means clustering were used in the case of no band selection;(e) Single-band iterative algorithm and FCM clustering were used in the case of no band selection;(f) Proposed method.

TABLE 2. The multi-spectral image change detection results evaluated by different algorithms.

Method Used	OE	PCC	KC	Time(s)
MAD	29044	0.819	0.161	0.713
IR-MAD	19015	0.881	0.245	1.854
With Mask	9924	0.938	0.376	2.860
SBIW(k-mean)	5971	0.963	0.531	3.257
SBIW(FCM)	7972	0.950	0.470	4.541
Proposed Method	5273	0.967	0.533	1.639

The detection results of IR-MAD and masking elimination method are improved, but the noise is more, and the change region is still not well distinguished. The two comparison algorithms of single-band iterative weighting algorithm and the proposed method have better detection results. By observing the objective evaluation indexes in Table 2, the total error number OE of MAD algorithm and IR-MAD algorithm is obviously higher, and the accuracy PCC and KAPPA values are lower. The detection accuracy of IR-MAD method was improved after adding mask, but it still could not detect the details well. In contrast, the single-band iterative weighting algorithm can detect the detail change information well. After comparing the three methods, it can be seen that the total error number OE will be lower after the band selection, and the correct rate PCC and KAPPA values are higher, indicating that the detection accuracy can be improved after the band selection. In terms of time complexity, MAD algorithm does not require the lowest iteration time complexity, but in terms of accuracy PCC and KAPPA values, MAD algorithm has low detection accuracy. This algorithm has low time complexity and the highest accuracy, so it has better change detection ability.

C. EXPERIMENTAL DATE III

Data III taken in changji region of xinjiang were selected for the experiment. The time-phase one image is a multispectral

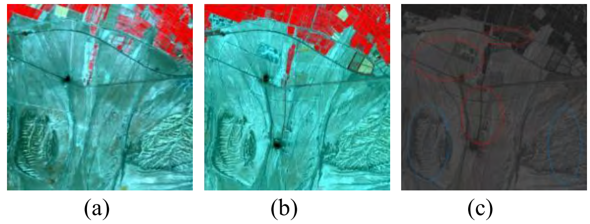

FIGURE 10. Pseudo-color composite image of multi-spectral data in Changji, Xinjiang: (a) 2011 and (b) 2014; (c) labeled reference area.

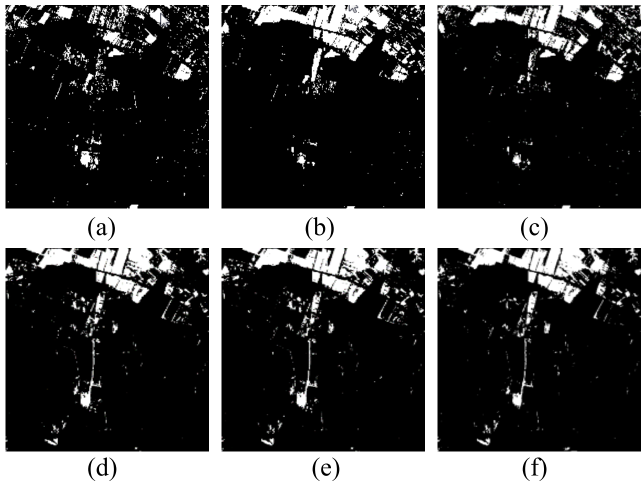

FIGURE 11. Change detection image obtained for the Changji simulated data set: (a) MAD; (b) IR-MAD; (c) masking to eliminate strong changes; (d) Single-band iterative algorithm and K-means clustering were used in the case of no band selection;(e) Single-band iterative algorithm and FCM clustering were used in the case of no band selection;(f) Proposed method.

image taken by landsat5-tm in 2011. There are seven bands in total, and six visible and near-infrared bands, except for the thermal infrared band (TM6), were selected. During phase 2 of the images taken in 2014 by landsat8-OLI [30] multispectral figure, there were a total of 11 bands, which were chosen corresponding with the cross section (Band 2), green band (Band 3), red band (Band 4), near infrared band (Band 5), short infrared band 1 (Band 6), and short infrared band 2 (Band 7). Then, the original image was geometrically registered, and the extract area of 500×500 pixels was used as the research object. As shown in Fig. 10, (a) presents the standard false color image synthesized in Band 4 (red band), Band 3 (green band), and Band 2 (blue band) in the multispectral image taken by landsat5-TM in 2011. In (b), a standard false color image synthesized in Band 5 (near-infrared), Band 4 (red band), and band 3 (green band) in a multispectral image taken by landsat8-OLI in 2014 is shown. In order to facilitate the comparison of the test results, a typical area was selected for comparison, as shown in Fig. 10 (c), in which the red mark represents the change area, while the blue mark represents the unchanged area.

As can be seen from the detection results in Fig. 11, the MAD algorithm, IR-MAD algorithm and masking strong change elimination method have poor ability to detect detail changes, and the detection results have more noise. The

TABLE 3. **The multi-spectral image change detection results evaluated by different algorithms.**

Method Used	Time(s)
MAD	1.238
IR-MAD	2.354
With Mask	3.151
SBIW(k-mean)	5.654
SBIW(FCM)	6.565
Proposed Method	2.557

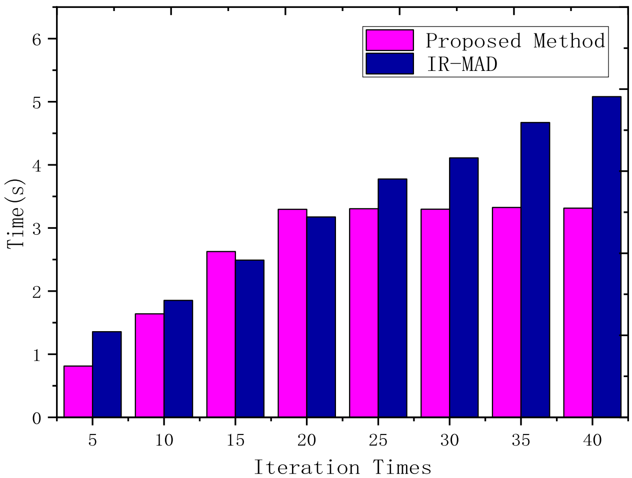

FIGURE 12. **Time complexity versus number of iterations.**

two comparison algorithms of single-band iterative weighting algorithm and the proposed method have better detection results, more accurate detection of detail changes, and less noise. According to Table 3, band selection can better reduce the time complexity and improve the efficiency of change detection. Through the experiments of the above three sets of data sets, the advantages of the single-band iterative weighting algorithm are verified, and the experiment proves that the band selection can avoid the influence of the band with less change information on the change detection result and reduce the time complexity. Therefore, this algorithm has better change detection ability.

IV. DISCUSSION

This section discusses our proposed algorithm from two aspects of time complexity and universality. In terms of time complexity, 30 groups of real multi-spectral remote sensing images were selected in this paper to calculate the detection time of IR-MAD algorithm and the proposed method under different iteration ltimes, and the histogram was drawn as shown in Fig. 12. It can be seen from the figure that the proposed method converges faster. In the case of fewer or more iterations, it has significant advantages. In other cases, the time complexity of the IR-MAD algorithm was increased by about 0.2 seconds. Therefore, in consideration of the same convergence condition, the proposed method has a lower time complexity.

From the perspective of universality: in this paper, 30 sets of landsat5-tm data sets were made by manually adding change areas. The change detection was carried out with the proposed method, and the comparison was made with the original MAD algorithm, IR-MAD algorithm and the proposed IR-MAD algorithm using mask to eliminate strong change. The mean values of PCC and KAPPA of the 30 data sets were obtained, and the results were shown in table 4.

TABLE 4. **Results of detecting the average change of multi-spectral remote sensing images.**

Method Used	$\overline{OE}$	$\overline{PCC}$	$\overline{KC}$
MAD	395	0.984	0.937
IR-MAD	308	0.988	0.952
With Mask	228	0.991	0.962
Proposed Method	75	0.997	0.988

As can be seen from Table 4, the average total error detection number OE of our proposed algorithm is the lowest. As can be seen from the average value of PCC and KAPPA, the single-band iterative weighting method is superior to other algorithms in detection accuracy. Through experiments on 30 sets of data, the advantages of this algorithm are fully verified, so the algorithm has good universality.

V. CONCLUSION

In this paper, a new multi-spectral change detection method based on band selection and single-band iterative weighting is proposed. Firstly, the bands with more change information are selected by calculating the characteristic canonical correlation between remote sensing image wavebands. In order to avoid the influence of the bands with more background and noise information on the change detection results. Secondly, the single-band iterative weighting algorithm is used to obtain the difference map. The original IR-MAD algorithm is improved to better enhance the correlation coefficient of each band, which could minimize the radiation difference contained in the unchanged pixel. so as to highlight the real changing ground objects in the difference by minimizing the radiation difference. Finally, the simple k-means clustering algorithm is used for binary clustering to obtain the detection results. The performance of the proposed method is compared with three existing methods: MAD, IR-MAD and the masking elimination method. The results show that the proposed algorithm can improve the accuracy of change detection and has good universality. The time required for the algorithm is related to the number of iterations, the image size, and the number of pixels in the image change. Considering the same convergence, the proposed method has lower time complexity.

REFERENCES

[1] M. Song, Y. Zhong, and A. Ma, "Change detection based on multi-feature clustering using differential evolution for Landsat imagery," *Remote Sens.*, vol. 10, no. 10, p. 1664, 2018.
[2] H. Zhuang, K. Deng, Y. Yang, and H. Fan, "An approach based on discrete wavelet transform to unsupervised change detection in multispectral images," *Int. J. Remote Sens.*, vol. 38, no. 17, pp. 4914–4930, 2017.
[3] Q. Luo, P. Wang, and W. Yong, "Study on a kind of land-use change detection based on patch objects of remote sensing image," in *Proc. Int. Conf. Inf. Sci. Technol.*, Mar. 2011, pp. 493–495.

[4] Z. Gao, N. Xu, C. Fu, and J. Ning, "Evaluating drought monitoring methods using remote sensing: A dynamic correlation analysis between heat fluxes and land cover patterns," *IEEE J. Sel. Topics Appl. Earth Observ. Remote Sens.*, vol. 8, no. 1, pp. 298–303, Jan. 2015.

[5] A. O. Yan-Hong, H. Pei, Y. L. Wang, and L. I. Yun-Peng, "Monitoring on land cover dynamics of hunshandake sandland by remote sensing," *J. Desert Res.*, vol. 30, no. 1, pp. 33–39, 2010.

[6] H. Zhuang, K. Deng, H. Fan, and S. Ma, "A novel approach based on structural information for change detection in SAR images," *Int. J. Remote Sens.*, vol. 39, no. 8, pp. 2341–2365, 2018.

[7] F. Wang and Y. J. Xu, "Comparison of remote sensing change detection techniques for assessing hurricane damage to forests," *Environ. Monitor. Assessment*, vol. 162, pp. 311–326, Mar. 2010.

[8] A. Shi, G. Gao, and S. Shen, "Change detection of bitemporal multispectral images based on FCM and D-S theory," *EURASIP J. Adv. Signal Process.*, vol. 2016, p. 96, Sep. 2016.

[9] C. Qiang and Y. Chen, "Multi-feature object-based change detection using self-adaptive weight change vector analysis," *Remote Sens.*, vol. 8, no. 7, p. 549, 2016.

[10] C. Yonezawa, "Maximum likelihood classification combined with spectral angle mapper algorithm for high resolution satellite imagery," *Int. J. Remote Sens.*, vol. 28, no. 16, pp. 3729–3737, 2007.

[11] H. Hichri, Y. Bazi, N. Alajlan, and S. Malek, "Interactive segmentation for change detection in multispectral remote-sensing images," *IEEE Geosci. Remote Sens. Lett.*, vol. 10, no. 2, pp. 298–302, Mar. 2013.

[12] J. Zhang and G. Yang, "Automatic land use and land cover change detection with one temporary remote sensing image," *J. Remote Sens.*, vol. 9, no. 3, p. 294, 2005.

[13] X. Lu, S. Zhang, Z. He, and G. Yan, "The comparative study of three methods of remote sensing image change detection," in *Proc. Int. Conf. Geoinformatics*, Aug. 2009, pp. 1–4.

[14] F. Bovolo and L. Bruzzone, "A theoretical framework for unsupervised change detection based on change vector analysis in the polar domain," *IEEE Trans. Geosci. Remote Sens.*, vol. 45, no. 1, pp. 218–236, Jan. 2007.

[15] H. W. Zhang, "A SAR image change detection algorithm based on principal component analysis," *J. Electron. Inf. Technol.*, vol. 30, no. 7, pp. 1727–1730, Jul. 2008.

[16] M. Bai, H. P. Liu, S.-D. Zhu, and H. H. Feng, "Relative radiometric correction for remote sensing images based on multivariate alteration detection," *Sci. Surveying Mapping*, vol. 37, no. 4, pp. 143–146, 2012.

[17] W. K. Härdle and Z. Hlávka, "Canonical Correlation Analysis," *J. Financial Econ. Policy*, vol. 6, no. 2, pp. 179–196, 2012.

[18] M. S. Liao, P. Zhu, and J. Y. Gong, "Multivariate change detection based on canonical transformation," *J. Remote Sens.*, vol. 4, no. 3, pp. 226–231, Aug. 2000.

[19] M. J. Canty and A. A. Nielsen, "Automatic radiometric normalization of multitemporal satellite imagery with the iteratively re-weighted MAD transformation," *Remote Sens. Environ.*, vol. 112, no. 3, pp. 1025–1036, Mar. 2008.

[20] A. A. Nielsen and M. J. Canty, "Kernel principal component and maximum autocorrelation factor analyses for change detection," *Proc. SPIE*, vol. 7477, Sep. 2009, Art. no. 74770T.

[21] I. Niemeyer, P. R. Marpu, and S. Nussbaum, "Change detection using object features," in *Object-Based Image Analysis*. Berlin, Germany: Springer, 2008.

[22] P. R. Marpu, P. Gamba, and M. J. Canty, "Improving change detection results of IR-MAD by eliminating strong changes," *IEEE Geosci. Remote Sens. Lett.*, vol. 8, no. 4, pp. 799–803, Jul. 2011.

[23] C. Wu, B. Du, and L. P. Zhang, "Research on multi-level information change detection of remote sensing images," Ph.D. dissertation, Dept. Elect. Eng., Wuhan Univ., Wuhan, China, 2015.

[24] Q. Xu, Z. Liu, F. Li, H. Ren, and M. Yang, "The regularized iteratively reweighted object-based MAD method for change detection in bi-temporal, multispectral data," *Proc. SPIE*, vol. 10156, Oct. 2016, Art. no. 101560P.

[25] Y.-Q. Cheng, H.-C. Li, T. Celik, and F. Zhang, "FRFT-based improved algorithm of unsupervised change detection in SAR images via PCA and K-means clustering," in *Proc. IEEE Int. Geosci. Remote Sens. Symp. (IGARSS)*, Jul. 2014, pp. 1952–1955.

[26] G. Feng, X. Liu, J. Dong, G. Zhong, and M. Jian, "Change detection in SAR images based on deep semi-NMF and SVD networks," *Remote Sens.*, vol. 9, no. 5, p. 435, 2017.

[27] P. R. Leal, J. C. Froment, and M. Sindou, "[MRI sequences for detection of neurovascular conflicts in patients with trigeminal neuralgia and predictive value for characterization of the conflict (particularly degree of vascular compression)]," *Neuro-Chirurgie*, vol. 56, no. 1, pp. 43–49, 2010.

[28] M. Gong, Z. Zhou, and J. Ma, "Change detection in synthetic aperture radar images based on image fusion and fuzzy clustering," *IEEE Trans. Image Process.*, vol. 21, no. 4, pp. 2141–2151, Apr. 2012.

[29] D. Sulla-Menashe, M. A. Friedl, and C. E. Woodcock, "Sources of bias and variability in long-term Landsat time series over Canadian boreal forests," *Remote Sens. Environ.*, vol. 177, pp. 206–219, May 2016.

[30] X. U. Wei and X. I. Yan-Tao, "Research on land use classification in Hefei based on Landsat8 images," *Hubei Agricult. Sci.*, vol. 54, no. 15, pp. 3625–3629, 2015.

LIYUAN MA received the bachelor's degree in electronic information engineering from the School of Information Science and Engineering, Xinjiang University, China, in 2017, where she is currently pursuing the master's degree. Her research direction is digital image processing.

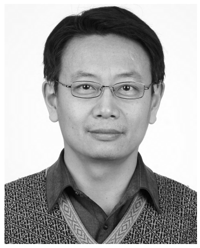

ZHENHONG JIA received the B.S. degree from Beijing Normal University, Beijing, China, in 1985, and the M.S. and Ph.D. degrees from Shanghai Jiao Tong University, Shanghai, China, in 1987 and 1995, respectively. He is currently a Professor with the Autonomous University Key Laboratory of Signal and Information Processing Laboratory, Xinjiang University, China. His research interests include digital image processing, photoelectric information detection, and sensor.

YINFENG YU received the bachelor's and master's degrees from Xinjiang University, China, in 2008 and 2011, respectively. He is currently pursuing the Ph.D. degree in computer science with Tsinghua University. His research interests include image processing, computer vision, and natural language processing.

JIE YANG received the Ph.D. degree from the Department of Computer Science, Hamburg University, Germany, in 1994. He is currently a Professor with the Institute of Image Processing and Pattern Recognition, Shanghai Jiao Tong University, China. His major research interests include object detection and recognition, data fusion and data mining, and medical image processing.

NIKOLA K. KASABOV (M'93–SM'98–F'10) received the M.S. degree in computing and electrical engineering and the Ph.D. degree in mathematical sciences from the Technical University of Sofia, Sofia, Bulgaria, in 1971 and 1975, respectively. He is currently the Director and the Founder of the Knowledge Engineering and Discovery Research Institute and a Professor of knowledge engineering with the School of Computing and Mathematical Sciences, Auckland University of Technology, Auckland, New Zealand. His major research interests include information science, computational intelligence, neural networks, bioinformatics, and neuroinformatics.